Structural Basis for the Photochemistry of α-Phycoerythrocyanin[†,‡]

Marius Schmidt,*[,§] Anamika Patel,[§] Yi Zhao,[§] and Wolfgang Reuter*[,||]

Physikdepartment E17, Technische Universität München, James Franck Strasse, 85747 Garching, Germany, and Max Planck Insititut für Biochemie, Am Klopferspitz 18A, 82152 Martinsried, Germany

Received September 4, 2006; Revised Manuscript Received November 7, 2006

ABSTRACT: Phycobiliproteins and phytochromes are light-harvesting and light-sensing proteins containing linear tetrapyrroles, so-called bile chromophores. The chromophores in certain biliproteins, including the phytochromes, isomerize reversibly from a stable *Z*-configuration to a stable *E*-configuration when irradiated with light of the appropriate wavelength. Here, we report the crystal structure of α-phycoerythrocyanin with its chromophore in the *E*-configuration, compare it with the *Z*-configuration found in trimeric phycoerythrocyanin, and reveal the structural bases of the isomerization. The geometric changes of the chromophore account for the large spectral shift, which characterizes the overall transition. Interactions of the chromophore A and D pyrrole rings with flexible protein moieties are required for the formation and stabilization of the isomers. We predict that the results will hold for all photoactive biliproteins.

Light is the most prominent factor that directly and indirectly drives and regulates various biological processes in living organisms (*1*−*3*). Diverse classes of protein−chromophore complexes involved in photosynthesis, light protection, and light perception have evolved.

The light-harvesting antennae of photosynthetic cyanobacteria and red algae consist of proteins containing linear tetrapyrroles known as bile chromophores. Together with linker proteins, they are assembled into phycobilisomes, which absorb light and transfer the energy step by step to the photosynthetic reaction centers (*4*). The phycoerythrocyanin (PEC)[1] in phycobilisomes of certain cyanobacteria (*4*−*6*) contains α-subunits (α-PEC), each of which has a single, covalently attached phycoviolobilin (PVB) chromophore. PVB (Figure 1A) is converted from phycocyanobilin (PCB) by a lyase with two heterologous subunits (*7*) and then attached to helix 5 of α-PEC at position Cys84 (Figure 1B,C). The PVB chromophore is photoactive and undergoes the typical *Z*- to *E*-isomerization (*8*) (Figure 1A). The trimeric PEC of *Mastigocladus laminosus* consists of three $\alpha\beta$ heterodimers, $(\alpha\beta)_3$, and all three PVB chromophores reveal the ^{15}Z-configuration (*9*, *10*) (Figure 1B). Similar $(\alpha\beta)_3$ complexes are also found in the other phycobiliprotein classes of cyanobacteria and red algae, which are allophycocyanin (AP), phycocyanin (PC), and phycoerythrin (PE) (*11*), but distinct photoisomers could not be identified. The β-subunits of the trimeric PEC contain two PCB chromophores each (Figure 1B) that also do not form stable photoisomers, because ring D of the PCBs either is fixed by the protein environment or can rotate freely and may only be transiently photoactive (*10*). In the trimeric state, the photoreactivity of α-PEC is strongly suppressed by interactions with neighboring subunits (*12*), whereas the isolated α-subunit is fully photoactive (*8*). Excitation of the α-subunit in the *E*-configuration at 500 nm shifts the absorption maximum to 567 nm of the *Z*-configuration, and vice versa (*8*, *13*). A prerequisite for the reversible *Z*- to *E*-isomerization of the PVB is a high protein flexibility (*10*, *14*), especially of the extended loop between helices H4 and H5.

Phytochromes also contain linear tetrapyrroles as their photoactive chromophores. The phytochromes act as photosensors in various photosynthetic and nonphotosynthetic organisms (*15*, *16*). The phytochromobilin (PΦB) chromophore in plants (*3*, *17*) may be replaced in other organisms by different bilins (*16*) such as biliverdin (BV). PΦB is photoactive when illuminated by light of the appropriate wavelength, which shifts its absorption maximum by ∼60 nm from 660 to 720 nm. As in α-PEC, this reaction is reversible and has been attributed to isomerization around the C15═C16 bond between pyrrole rings C and D of the bilin, where ring D can adopt either the *Z*- or *E*-configuration (*18*). Consequently, α-PEC serves as a model for the photoreaction in phytochromes and phycobiliproteins in general, since the photochemical reactions of the chromophores are identical (*13*, *18*).

No structural basis for following this isomerization within the protein environment exists. Here, we present the three-dimensional structure of an isolated phycobiliprotein subunit, that of α-PEC in the *E*-configuration (α_E-PEC). The comparison of this structure with that of α-PEC in the *Z*-configuration (α_Z-PEC) (*9*, *10*) identifies the structural basis

[†] This work was supported by SFB-533 of the Deutsche Forschungsgemeinschaft.

[‡] The coordinates for the α_E-PEC have been deposited in the Protein Data Bank as entry 2j96.

* To whom correspondence should be addressed. M.S.: Physikdepartment E17, Technische Universität München, James Franck Strasse, 85747 Garching, Germany; telephone, +49-(0)89-2891-2550; fax, +49-(0)89-2891-2548; e-mail, marius.schmidt@ph.tum.de. W.R.: Max Planck Insititut für Biochemie, Am Klopferspitz 18A, 82152 Martinsried, Germany; e-mail, w.reuter@online.de.

[§] Technische Universität München.

[||] Max Planck Insititut für Biochemie.

[1] Abbreviations: AP, allophycocyanin; BV, biliverdin; DBV, dihydrobiliverdin; PC, phycocyanin; PCB, phycocyanobilin; PE, phycoerythrin; PEC, phycoerythrocyanin; PUB, phycourobilin; PVB, phycoviolobilin; PΦB, phytochromobilin; *E*, Entfernt, trans; *Z*, Zusammen, cis.

10.1021/bi061844j CCC: $37.00
Published on Web 12/15/2006

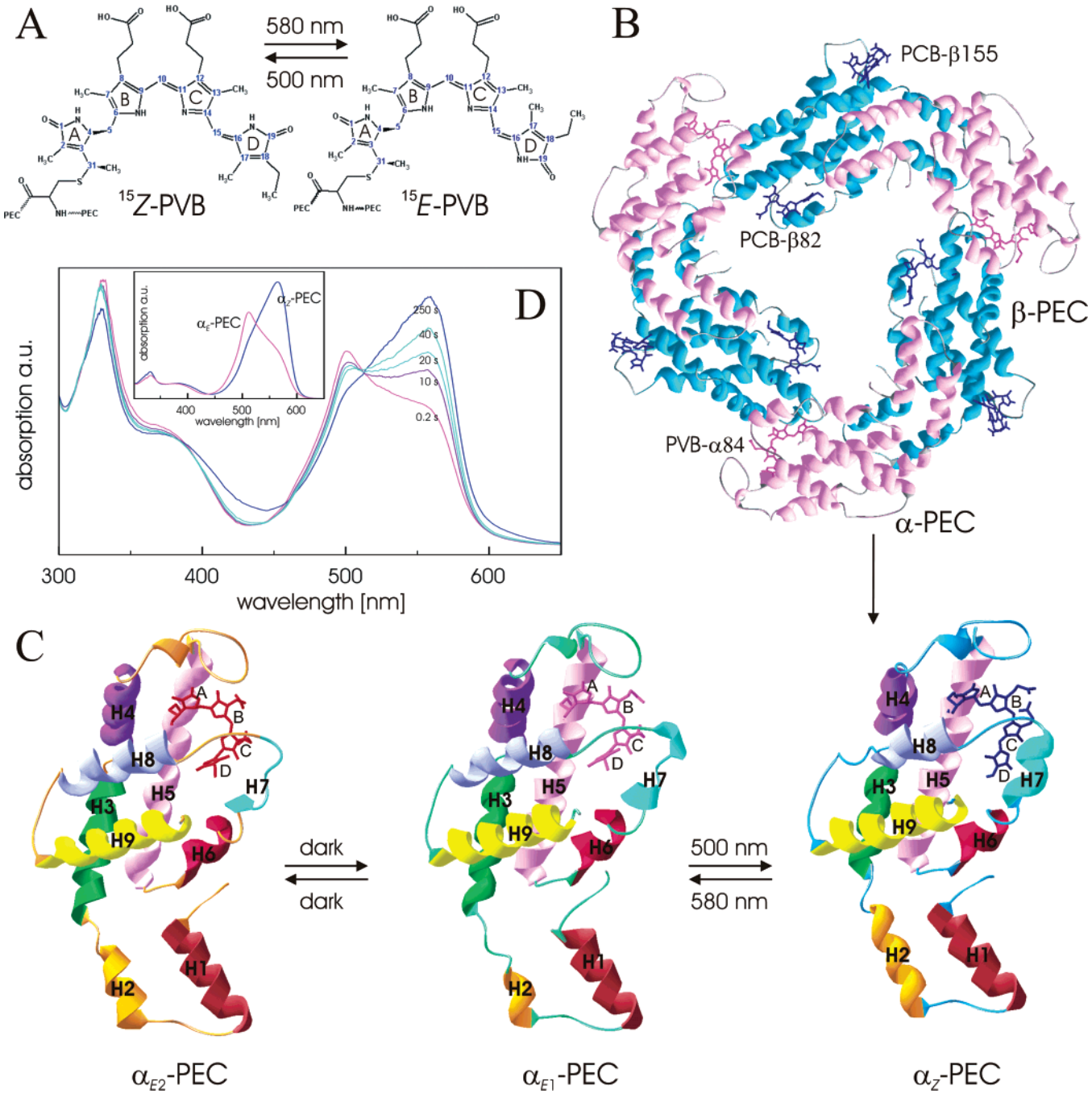

FIGURE 1: Structures and corresponding absorption spectra of α_E-PEC and α_Z-PEC. (A) Chemical structures of PVB: (left) *Z*-configuration and (right) *E*-configuration. The wavelengths that drive the transitions are marked near the arrows. (B) Three-dimensional structure of $(\alpha\beta)_3$-PEC: pink for α-PEC and blue for *β*-PEC. One of the three PVBs (dark pink) at position α84 and two of the six PCBs (dark blue) at positions *β*82 and *β*155 are marked. (C) Crystal structures of α_Z-PEC, α_{E1}-PEC, and α_{E2}-PEC. The nine helices are marked. ^{15}*Z*-PVB is colored blue in α_Z-PEC, and ^{15}*E*-PVB is colored pink and red in α_{E1}-PEC and α_{E2}-PEC, respectively. The wavelengths that drive the transitions are marked near the arrows. (D) Absorption spectra of α-PEC obtained from the crystal at various times of illumination with white light. The inset shows the absorption spectra of α-PEC obtained in 0.3% (v/v) formic acid (pH 2.1).

of the *Z*- to *E*-isomerization. By comparing the new results for α-PEC to spectroscopic and structural data of other phycobiliproteins, we explore the essential interrelation of natural chromophore structures, chromophore−protein interactions, and spectroscopic behaviors.

MATERIALS AND METHODS

Crystallization. Trimeric and hexameric phycoerythrocyanin complexes have been obtained from phycobilisomes of *M. laminosus* (*19*). The PVB containing, photoactive α-subunit was isolated and purified from $(\alpha\beta)_3$-PEC as described previously (*14*). To store the α-subunit without any degradation and aggregation, the proteins were bound in 1.0 mol/L potassium phosphate (pH 7.0) to isopropyl-substituted Sephacryl S-300 (Pharmacia), which was also used for the separation of the subunits from the trimer. After elution of α-PEC from the gel with 0.3% (v/v) formic acid, a buffer exchange and the final purification of the sample were obtained by gel filtration on a Superdex G75 column (Pharmacia) in 25 mM potassium phosphate (pH 7.0).

Table 1: Data Collection and Refinement Statistics for α_E-PEC

space group	*C*2
unit cell	$a = 129.8$ Å, $b = 102.6$ Å, $c = 32.1$ Å, $\alpha = 90°$, $\beta = 95.4°$, $\gamma = 90°$
resolution (Å)	2.25
completeness (%)	90.8
$I/\sigma I$ (last shell)	4.2 (2.0)
R_{sym} (last shell) (%)	6.9 (24.9)
R_{cryst}/R_{free}, molecular replacement (%)	42.5/48.5 at 3.2 Å
R_{cryst}/R_{free}, final model (%)	23.4/29.8
no. of H_2O molecules	444
B-values averaged over rings A/B/C/D	
α_{E1}-PEC PVB (Å^2)	26.3/30.1/29.4/36.3
α_{E2}-PEC PVB (Å^2)	27.7/25.0/26.3 /37.4
α_Z-PEC PVB [110 K (*10*)] (Å^2)	37.4/36.4/31.9/29.6

α_E-PEC was crystallized at 18 °C with the hanging drop method mixing 2 μL of 10 mg/mL protein with an equal amount of reservoir solution containing 1.2 mol/L potassium phosphate (pH 7.0) and 0.2 mol/L $MgSO_4$. Immediately after the plates were set up, they were irradiated for 1 h with an array of 12 high-power light-emitting diodes (OSRAM LY 5415-CW, typ.1120 mlm each) emitting 587 nm light. After 5 days, needle-shaped crystals appeared in the space group *C*2 ($a = 129.8$ Å, $b = 102.6$ Å, $c = 32.1$ Å, $\alpha = 90°$, $\beta = 94.5°$, and $\gamma = 90°$). These crystals were soaked in 1.2 mol/L potassium phosphate (pH 7.0) and 0.2 mol/L $MgSO_4$ with a cryoprotectant of 20% (w/v) sucrose before being flash-frozen in a nitrogen stream and structure analyses at 110 K. The same buffer including the sucrose was used for the spectroscopic measurements of the crystals at 268 K.

Structure Determination. An initial data set was collected at 110 K to 2.5 Å resolution under a safe light of 650 nm. The recently determined structure of the α_Z-subunit within the natural trimeric assembly [Protein Data Bank (*20*) entry 2c7l] served as search model for molecular replacement using Beast (*21*). The model was adjusted manually into the electron density using Xfit (*22*). Subsequently, the structure was refined (*23*) at 2.25 Å resolution using synchrotron data from beam line X13 at EMBL/Desy Hamburg. Data and refinement statistics are given in Table 1. The PVB chromophore was included in the refinement, and restraints for the PVB were generated as described previously (*10*). PVB restraints, which refer to the sp_3-hybridized C4 and C5 atoms, were weakened to allow some deviation from the expected tetrahedral geometry. The final model includes two α-subunits with 162 amino acids each and 445 water molecules in the asymmetric unit. The final R_{work} was 23.4% and R_{free} 28.9% for the data to 2.25 Å.

Spectroscopic Measurements. The absorption spectra of monomeric α-PEC in solution were recorded in 0.3% (v/v) formic acid (pH 2.1) that prevents the association and aggregation of the protein. The absorption spectra of the crystals were recorded with a microspectrophotometer located at the ESRF/Fr (*24*). A typical α_E-PEC crystal (100 μm × 50 μm × 50 μm) in cryo buffer was looped and mounted at −5 °C. All manipulations were performed in dim, white light of the lowest possible intensity in a dark room. The CCD detector of the spectrophotometer recording the spectra was started before the crystal was illuminated. The opening of the shutter of the Xe lamp produced a spot of 20 μm (full width at half-maximum) on the crystal. Entire spectra were recorded within 300 ms, each. The photoisomerization within the crystals driven by the measuring light was recorded up to 250 s. After this time, no changes in the absorption ratio of 510 nm to 567 nm could be detected.

Effective Length of a Conjugated π-System. A free electron molecular orbital (FEMO) calculation takes into account the length of a system of conjugated double bonds (*25*). It cannot, however, be used to explain absorption changes due to geometric distortions. Unless precise quantum mechanical calculations are available on the chromophore, a more empirical method must be used. The term "effective length" originates from the idea that a distorted, nonplanar geometry decouples a part of the conjugated system of double bonds and makes it virtually shorter. For bile chromophores, the system of double bonds extends roughly parallel to the shortest main axis of inertia that can be determined easily once the three-dimensional (3D) structure of the chromophore is known. The shortest main axis of inertia is that axis about which the free chromophore rotates most easily. Its direction is usually parallel to a vector connecting ring A with ring D. Accordingly, the effective length of a bilin can be calculated by projecting the conjugated bonds to its shortest main axis of inertia (ELcalc, available from the authors; see the Supporting Information). The 3D structures of a number of bilins were selected from various X-ray structures of the Protein Data Bank, and the absorption maxima of the different phycobiliproteins were obtained from the literature. Effects by excitonic coupling between chromophores were excluded by selecting the spectral properties of noncoupled chromophores (see the Supporting Information). Biliverdin (BV) in *DrBph* was not taken into account, because it is not in its extended form but rather exhibits a curved shape (*26*). The absorption maxima were plotted as a function of the calculated effective length and fitted by a straight line. Hence, the effective length of a bile chromophore whose 3D structure is unknown can be estimated by its absorption maximum. Vice versa, if the structure of a chromophore is known, its absorption maximum can be predicted.

RESULTS

Overall Architecture of Phycoerythrocyanin. Figure 1 gives an overview of the spectral and structural properties of PEC and connects our new structure of α_E-PEC with that of α_Z-PEC. The structure of the native PEC ring is shown in Figure 1B. Here, the α- and β-subunits interact via their two N-terminal helices, H1 and H2, and three of these $\alpha\beta$ heterodimers (called monomers by convention) associate into a disklike structure in which helices H4 and H5 of the α-subunits in one heterodimer interact with helices H6 and H7 of the β-subunits of a neighboring heterodimer. Here, only the photoactive α-subunit (α-PEC), which consists of nine helices (Figure 1C), is described in more detail.

α_E-PEC Assembly. The α-PEC subunits in the *E*-configuration crystallize in monoclinic space group *C*2 with two structurally distinct subunits, which we denote α_{E1}-PEC and α_{E2}-PEC in the asymmetric unit. Indeed, analytical ultracentrifugation and light scattering experiments revealed a high content of α_2 dimers in solution (W. Reuter, unpublished results). As in the heterodimers of the native PEC disks, the assembly of α_E-PEC arises from interactions between helices H1 and H2 of one α-PEC with helices H3 and H5 of the

other. However, these homodimers are not able to form the trimeric rings. Figure 1C compares the structures of α_{E1}-PEC and α_{E2}-PEC with that of α_Z-PEC within the functional $(\alpha\beta)_3$ trimer. The overall structures are similar but differ markedly in helices H2, H4, H7, and H8, and in their neighboring loops. The $\alpha_{E1}\alpha_{E2}$ dimer is kept together predominantly by hydrophobic interactions. However, the interface between the subunits is highly symmetric. In each subunit there are two tyrosins, Tyr18 and Tyr97, which form hydrogen bonds with Ser17 and Asp89 of the other subunit, respectively, and four interactions result. These tyrosins act like an anchor to orient the subunits in the mentioned symmetric way. There are no further specific interactions.

Photochemistry of α*-PEC.* Figure 1D (insert) shows the reversible absorbance shifts between maxima at 510 and 567 nm of isolated α-subunits when excited at 500 or 580 nm in solution. The spectrum of α_E-PEC exhibits a significant shoulder at 567 nm, similar to the low-wavelength shoulder of phytochromes in the $P_r(Z)$ state. The transition of α_E-PEC toward α_Z-PEC as well as the structural and spectral properties of α_E-PEC was correlated by microspectrophotometry on the crystals (Figure 1D). The absorption spectra of the crystals are directly comparable to those in solution. It has been suggested that the shoulder in the spectrum of α_E-PEC reflects an incomplete transition from the *Z*- to *E*-state (*8*, *12*) with some molecules still in the Z-configuration. However, in the α-PEC crystals, such a mixture is difficult to identify. The $F_{obs} - F_{calc}$ difference maps are flat, if inspected at the ring D position of the *Z*-form. Hence, the shoulder likely is of another origin (see below). The spectra in Figure 1D show the transition to the *Z*-state, which is complete in 250 s under our experimental conditions. This demonstrates that complete isomerization takes place within the crystals, which will be important for future time-resolved crystallographic studies (*27*−*29*). Although the isomerization was driven by continuous illumination with white light that excites the crystal at both effective wavelengths, the *E*-state is almost completely shifted into the *Z*-state. The slight shoulder at 510 nm in the final spectrum indicates that only a small proportion of α_E-PEC remains. This suggests that the molecules are more stable in the *Z*-configuration. High absorption values near 330 nm were also found in denatured phycobiliprotein subunits (*5*, *30*, *31*). In our case, they not only might reflect the part of subunits, which are just relaxing to either the *Z*- or *E*-configuration, but also might contain effects coming from the fixed orientation of the single crystal toward the measuring light (*32*).

Mechanism of the Z- to E-Transition. Figure 2A,B shows the structure of the chromophore and its protein environment in the *E*- and *Z*-configurations. In α_Z-PEC, the PVB is in its extended configuration, whereas in α_E-PEC, isomerization has occurred about the Δ15,16 bond between rings C and D. However, ring D has rotated around the 14,15 single bond, lying about 90° out of the plane formed by rings B and C (the B−C plane). Hence, the normal to the B−C plane is almost perpendicular to that of ring D. Figure 2C demonstrates that a rotation around the 14,15 single bond can move ring D back into the B−C plane. Then, the isomerization to the *E*-configuration is more evident due to the outward-pointing ring nitrogen. To prevent thermal re-isomerization to the *Z*-configuration, the chromophore conformation must be stabilized by the protein. Two regimes can be identified.

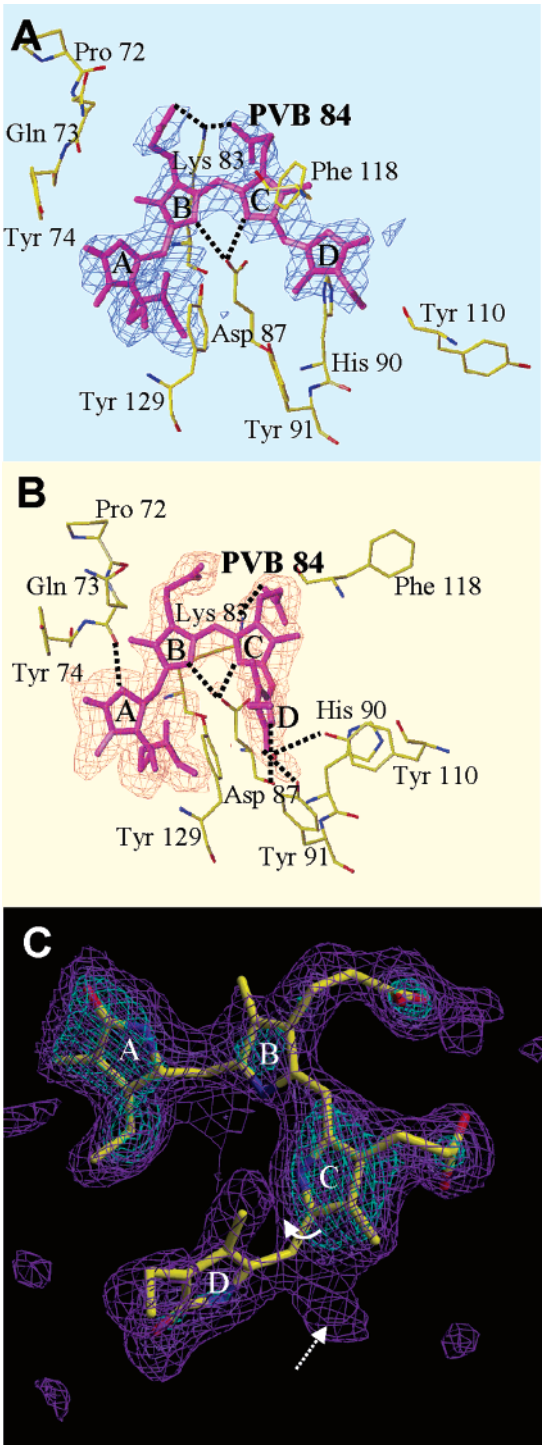

FIGURE 2: *Z*- to *E*-isomerization in α-PEC. Various amino acids in the surroundings of the chromophores are highlighted, and some important hydrogen bonds are shown as dotted lines: (A) PVB in the *Z*-configuration, electron density in blue; (B) PVB in the *E*-configuration, electron density in pink; and (C) structure of PVB covered by a simulated annealing omit map. The solid arrow shows that rotation about 14,15 single bond brings ring D into the B−C plane. The dotted arrow shows the density feature that might indicate a small contamination by the *Z*-isomer.

First, the H4−H5 loop that is close to PVB ring A changes its structure. The carbonyl oxygen of the Gln73 peptide bond forms a short hydrogen bond (2.85 Å) to the ring A nitrogen. Whereas in α_Z-PEC the H4−H5 loop is highly disordered (*10*), it is stabilized in α_E-PEC. Second, the end of helix 6 and the H6−H7 loop accommodate the major structural

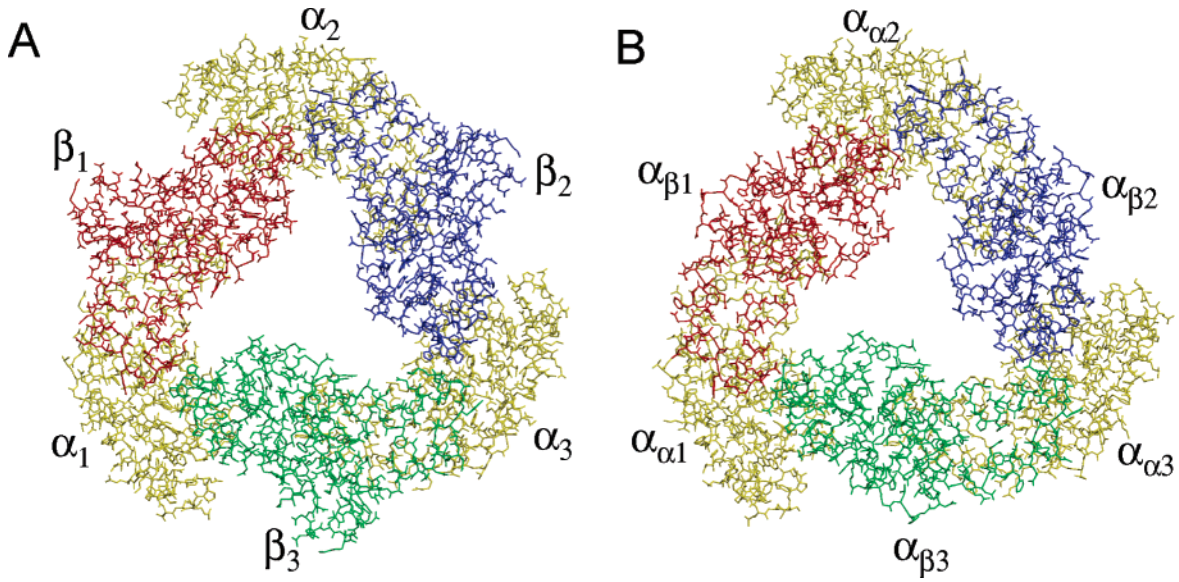

FIGURE 3: (A) Native trimeric PEC ring and (B) artificial $(\alpha_{E1}\alpha_{E2})_3$ ring.

changes around PVB ring D. In particular, aromatic residues Tyr110, Phe118, and His90 exhibit large displacements of up to 15 Å. They are directly involved in the mechanism of the isomerization and stabilization of α_E-PEC.

In the *Z*-isomer, PVB ring D is stabilized by hydrogen bonds only when the α-subunit interacts with a *β*-subunit of the neighboring heterodimer, which is the case in the $(\alpha\beta)_3$ trimer. However, even without a stabilizing hydrogen bond, the *Z*-isomer is the thermally stable form in freshly isolated α-subunits. Obviously, steric constraints with the protein hold ring D in place, as found for the PCB chromophores in *β*-PEC and most of the phycocyanins (*5*). Several amino acids contribute to the stabilization of the *E*-configuration (Figure 2). Most importantly, the PVB ring D carbonyl interacts with Tyr91 O_η by forming a new hydrogen bond that stabilizes the conformation of ring D. In addition, ring D forms a *π*-stack with Tyr129. Two slightly distinct PVB configurations are found in α_{E1}-PEC and α_{E2}-PEC. In α_{E1}-PEC, the ring D nitrogen interacts with a water molecule, which in turn is hydrogen bonded to Asp87 O and Tyr110 O_η. This interaction does not exist in α_{E2}-PEC. Nevertheless, the observed interactions are sufficient to prevent effective thermal re-isomerization to the *Z*-form. However, our results do not show whether an equilibrium of α_{E1}-PEC and α_{E2}-PEC is present in the dark or whether one of the structures represents an intermediate state on the pathway from the *Z*- to *E*-configuration.

The masses of the two α-subunits differ by 16 Da (data not shown). This difference does not arise during crystallization; it has also been reported in an earlier solution study (*14*). Presumably, one of the α_E-subunits is modified by oxidation. Although the presumed additional oxygen could not be localized, the modification of one of the subunits seems to be important for crystallization. These two distinct α_E-PECs may explain the slightly different *E*- to *Z*-transitions described previously as type I and type II photochemistry(*8*). Different intermediates on the reaction pathway can be expected for the two species (*13*, *18*, *33*).

DISCUSSION

Packing Effects. α_{E1} and α_{E2} are nearly identical. The root-mean-square distance difference between equivalent α-carbons is only 0.3 Å. Nevertheless, the structures of the two PVB chromophores are slightly different. The chromophores are directly involved in crystal packing contacts. The propionyl groups of the ^{15}*E*-PVBs orient in different ways in subunits A and B. Typically, distances across the borders of the asymmetric unit are larger for α_{E2}-PEC than for α_{E1}PEC. For this reason, Phe110, which is close to the chromphore at the protein−water interface, can point inward in α_{E2}-PEC but is rotated outward in α_{E1}-PEC. In subunit B, the chromophore ring D environment is therefore more hydrophobic, and this is probably the reason why no water is bound there (see the Supporting Information).

Figure 3A shows the native $(\alpha\beta)_3$-PEC ring in which the subunits are numbered $\alpha_N\beta_N$, where *N* runs from 1 to 3. It is evident that only the *β*-PEC subunits form a continuous ring with only one specific interaction (His75−Asp13) between the *β*-subunits. The α-subunits work like a clamp and bridge two adjacent *β*-subunits. Interactions between α-subunits do not exist. $\alpha_N\beta_N$ interactions are found in those subunits which constitute the asymmetric unit in native PEC crystals. $\beta_N\alpha_{N+1}$ interactions connect two adjacent αβ-blocks. Interactions involve the PVB chromophore and the two flanking regimes on both sides of the chromophore (see Table S2 and S3 of the Supporting Information for detailed distances). Since the subunits in $(\alpha_{E1}\alpha_{E2})$-PEC are arranged in a manner similar to that of $(\alpha\beta)$-PEC, we have oriented the $\alpha_{E1}\alpha_{E2}$-PEC structure as a rigid body onto the three native $(\alpha\beta)$-blocks forming an artificial trimeric ring (Figure 3B). The subunits are named α_α and α_β according to those of the native PEC. This ring helps to identify why (1) α-subunits alone do not form a ring, (2) α-PEC forms αβ heterodimers instead of αα homodimers in the presence of *β*-PEC, and (3) the subunits in αα-PEC are oriented in an almost identical fashion compared to the native αβ-PEC. (1) In the artificial ring, αβThr77 is found instead of βHis75 in the native structure. Interactions between the α_β-subunits similar to those in the native PEC ring do not exist. Prospective

interactions required for ring formation are greatly reduced in number, because pairs of residues that match are sparse. In addition, steric clashes occur between the H4−H5 loop (amino acids 60−82) in $\alpha_{\beta(N)}$ and the H7−H8 loop (amino acids 109−105) in $\alpha_{\alpha(N+1)}$. This prevents the α_a-subunits from clamping the ring structure together. (2) The number of specific interactions is small in αα-PEC. In αβ-PEC, this number is much higher, and αβ complexes are therefore more stable and will be strongly preferred when α- and β-subunits are present. (3) As mentioned above, the subunit interface in αα-PEC is highly symmetric. In αβ-PEC, this almost perfect symmetry does not exist due to sequence differences. Nevertheless, subunits in the αβ- and αα-dimers orient in the same way. The reason for this is that some of the tyrosins are rulers for the subunit orientation. For example, Tyr18 can be found in both α- and β-PEC. Each tyrosin finds a specific site around amino acid 90 in the adjacent subunit where it can interact. Another example is Tyr97 in α-PEC and Tyr95 in β-PEC, which find their mates at position 17 in the other subunit. Obviously, the tyrosines acting as bolts and complementary grooves exist to accommodate the bolts in well-preserved, almost identical distances either in α-PEC or in β-PEC. The bolts and grooves fit together, and the interfaces will orient in similar ways no matter which subunit is concerned. This interaction pattern can be found in many phycobiliproteins such as PC or AP through different species (*34*, *35*), and hybrid assemblies can therefore be anticipated.

Absorption Maxima of Bilins. α-PEC is a fully reversible photoswitch with a large number of prospective applications in diverse fields (*36*, *37*). It can be conveniently shifted between two stable isomeric forms, *Z* and *E*, with different spectral properties. Figure 1D shows the large shift in the absorption maximum when PVB isomerizes in either direction. If the chromophore would isomerize from an extended ^{15}*Z*-configuration to an extended ^{15}*E*-configuration, the length of the conjugated π-system would change only slightly. Therefore, only a small shift in the position of the absorption maximum should have been expected (see Materials and Methods). The question is why the shift is so large. In Figure 4, the positions of the absorption maxima of several biliproteins are plotted as a function of their effective length as defined in Materials and Methods. For the phycobilins, this plot is linear. This approach is quite sensitive. For example, the geometries and the effective lengths of the chemically identical PCB chromophores within the β-subunits of PEC differ slightly. Accordingly, slightly different absorption maxima near 600 nm are observed. Consequently, X-ray structures can be used to estimate the positions of the absorbance maxima of a single bilin chromophore within the protein environment. Data for α_E-PEC and α_Z-PEC lie on the line in Figure 4. We propose that both the number of conjugated bonds and the chromophore geometry have the largest influence on the position of absorption maxima. PVB in its *E*-configuration has an absorption maximum close to that of phycourobilin (PUB), whereas the absorption maxima of PVB in its Z-configuration and dihydrobiliverdin (DBV) are close, although the chemical structures of the chromophores are quite different. In ^{15}*E*-PVB, ring D is perpendicular to that of the B−C plane, which partially decouples ring D from the system of conjugated bonds and reduces the effective length of the chromophore to that of the PUB. However, the α_E-PEC shoulder at 567 nm may arise from

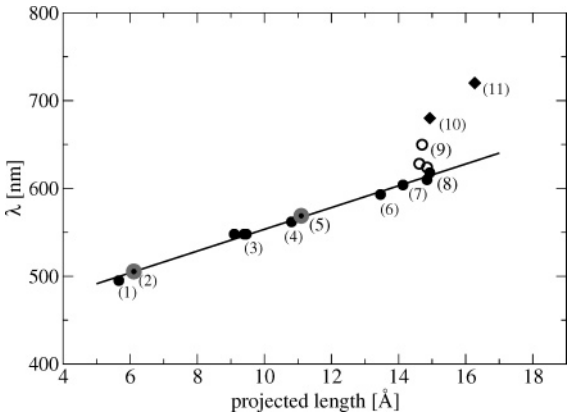

FIGURE 4: Absorption maxima of several bilins as a function of the effective length of their chromophores (see also the Supporting Information for details). α-PEC in its *Z*- and *E*-states is highlighted with circles: (1) phycourobilin, (2) ^{15}*E*-PVB in α_E-PEC (this work), (3) phycoerythrobilin, (4) dihydrobiliverdin, (5) ^{15}*Z*-PVB in α_Z-PEC, (6) phycocyanobilin-β155 in PEC, (7) phycocyanobilin-β84 in PEC, (8) phycocyanobilins in isolated α and β subunits of PC (own measurements) and phycocyanobilins in isolated α and β subunits of AP (own measurements), (9) excitonically coupled phycocyanobilins in PC and AP trimers (empty symbols), (10) PΦB$_r$ in plant phytochromes in the red-absorbing *Z*-configuration, with the chemical structure superimposed on the three-dimensional structure of ^{15}*E*-PVB, and (11) PΦB$_{fr}$ in plant phytochromes in the far-red-absorbing *E*-configuration with the chemical structure superimposed on the three-dimensional structure of ^{15}Z-PVB. The solid line is the result of a least-squares fit including only nonexcitonically coupled bilins.

incomplete decoupling, which occurs in some fraction of the α_E-PEC molecules in the crystalline ensemble. The higher *B* values of PVB ring D (Table 1) indeed provide evidence of such an inhomogeneity. In addition, the small electron density feature in Figure D (dotted arrow) might be an indication of a remaining *Z*-configuration. On the other side, the shoulder is much too pronounced to be caused only by such a minor fraction. Further spectroscopic experiments such as spectral hole burning (*38*) in solution and in the crystal should clarify the exact nature of this shoulder. Nevertheless, this shoulder can also be observed in the spectrum of the plant phytochrome species P_r, and geometric effects similar to those observed in ^{15}*E*-PVB can be anticipated for the PΦB chromophore there.

A Modified Hierarchy. A hierarchy of factors influences the absorbance of bilin-containing proteins. (1) The chemical structure accounts for the number of conjugated bonds, which roughly determines the position of the absorption maximum of chromophores. (2) The geometry of the chromophore strongly modifies this position. Shifts larger than 50 nm are possible, and in addition, shoulders can occur in the spectra as observed for α-PEC. (3) Excitonic coupling shifts the spectrum by up to 40 nm when certain chromophores come closer together. For example, this is the case when αβ heterodimers trimerize (Figure 1B). Two salient examples are AP and PEC. In AP, strong excitonic coupling shifts the absorption maximum from 615 to 651 nm (*39*), whereas in PEC, a shift in the opposite direction from 615 to 575 nm is observed (*40*). (4) Furthermore, chromophore protonation or interactions by hydrogen bonds may shift the absorbance maxima. Couplings with neighboring aromatic amino acids also have a large effect: in allophycocyanin B, a simple

replacement of a tyrosine with tryptophan shifts the absorbance maximum (*39*, *41*) by several tens of nanometers.

Consequence for the Phytochromes. The phytochromes do not fit to the linear relationship in Figure 3. Although their conjugated system of double bonds seems to be in the extended configuration (*42*), this is not sufficient to explain their unexpected red-shifted absorption maxima of around 660 and 720 nm for the P_r and P_{fr} states of PΦB, respectively. Since phytochromes bear a single chromophore, excitonic coupling can be excluded. We assume that their absorption at longer wavelengths is ascribed to interaction with aromatic amino acids extending the resonantly coupled π-system (*43*). Indeed, the recently published structure (*26*) of a bacterial (*Deinococcus radiodurans*) phytochrome fragment (*DrBph*) shows that its biliverdin (BV) chromophore interacts strongly with a number of phenylalanine residues. However, on the basis of the results for α-PEC, we can anticipate that the transitions from the *Z*- to *E*-configuration in both PΦB and BV are accompanied by large geometric rearrangements. In all phytochromes, a *Z*- to *E*-transition is accompanied by a shift in the absorbance to higher wavelengths, just contrary to PEC where a blue shift is observed. In the case of *DrBph*, the BV chromophore is found in its curved syn/syn/anti configuration in the *Z*-state (*26*) (see the Supporting Information). In this configuration, BV ring A is bent toward rings B and C and ring D is already extended. Therefore, an isomerization to the *E*-form might involve not only BV ring D but also the conformation and configuration of BV ring A leading to a more extended BV geometry and to an absorption at higher wavelengths.

CONCLUDING REMARKS

Taken together, the structural comparison of α_E-PEC with α_Z-PEC explores the *Z*- to *E*-transitions in biliproteins. The photochemistry in α-PEC is coupled to two regions, the H4−H5 and H7−H8 loops where large structural changes occur. The geometry of the chromophore influences its effective length, which determines the position of its absorption maximum and the shape of the entire spectrum. Further interactions of the chromophore with aromatic amino acids or by excitonic couplings can be predicted in this way. In addition, shoulders in absorption spectra such as those in the spectra of the P_r state of phytochrome or of α_E-PEC are explained. We postulate that in functional photosynthetic antennae geometric differences in chemically identical phycobilins are essential for the stepwise energy transfer within and between the phycobiliprotein complexes.

ACKNOWLEDGMENT

The help of Dominique Bourgeois with the microspectrophotometer is greatly appreciated. We thank Keith Moffat for reading and commenting on an earlier version of this paper. M.S. acknowledges perpetual support by Fritz Parak.

SUPPORTING INFORMATION AVAILABLE

Effective lengths and absorption maxima of the bile chromophores in tabular form and their chemical structures, the α_E-PEC dimer as it is lying in the asymmetric unit shown in stereo, details for interactions between symmetry-related subunits, and a short description of the program ELcalc are given. This material is available free of charge via the Internet at http://pubs.acs.org.

REFERENCES

1. Batschauer, A. (1998) Photoreceptors of higher plants, *Planta 206*, 479−492.
2. Cashmore, A. R., Jarillo, J. A., Wu, Y.-J., and Liu, D. (1999) Cryptochromes: Blue light receptors for plants and animals, *Science 284*, 760−765.
3. Briggs, W. R., and Olney, M. A. (2001) Photoreceptors in plant photomorphogenesis to date. Five phytochromes, two cryptochromes, one phototropin, and one superchrome, *Plant Physiol. 125*, 85−88.
4. Glazer, A. N. (1989) Light guides: Directional energy transfer in a photosynthetic antenna, *J. Biol. Chem. 264*, 1−4.
5. MacColl, R. (1998) Cyanobacterial Phycobilisomes, *J. Struct. Biol. 124*, 311−334.
6. Bryant, D. A. (1982) Phycoerythrocyanin and phycoerythrin. Properties and occurrence in cyanobacteria, *J. Gen. Microbiol. 128*, 835−844.
7. Storf, M., Parbel, A., Meyer, M., Strohmann, B., Scheer, H., Deng, M. G., Zheng, M., Zhou, M., and Zhao, K. H. (2001) Chromophore attachment to biliproteins: Specifity of PecE/PecF, a lyase-isomerase for the photoactive 3^1-Cys-α84-phycoviolobilin chromophore of phycoerythrocyanin, *Biochemistry 40*, 12444−12456.
8. Zhao, K.-H., and Scheer, H. (1995) Type I and type II reversible photochemistry of phycoerythrocyanin α-subunit from *Mastigocladus laminosus* both involve *Z*, *E* isomerization of phycoviolobilin chromophore and are controlled by sulfhydryls in apoprotein, *Biochim. Biophys. Acta 1228*, 244−253.
9. Duerring, M. R., Huber, R., Bode, W., Ruembeli, R., and Zuber, H. (1990) Refined three-dimensional structure of phycoerythrocyanin from the cyanobacterium *Mastigocladus laminosus* at 2.7 Å, *J. Mol. Biol. 211*, 633−644.
10. Schmidt, M., Krasselt, A., and Reuter, W. (2006) Local protein flexibility as a prerequisite for reversible chromophore isomerization in α-Phycoerythrocyanin, *Biochim. Biophys. Acta 1764*, 55−62.
11. Sidler, W. A. (1994) Phycobilisome and Phycobiliprotein Structures, in *The Molecular Biology of Cyanobacteria* (Bryant, D. A., Ed.) pp 139−216, Kluwer Academic Publishers, Dordrecht, The Netherlands.
12. Siebzehnrübl, S., Fischer, S. F., Kufer, W., and Scheer, H. (1989) Photochemistry of phycobiliproteins: Reciprocity of reversible photochemistry and aggregation in phycoerythrocyanin from *Mastigocladus laminosus*, *Photochem. Photobiol. 49*, 753−761.
13. Foerstendorf, H., Parbel, A., Scheer, H., and Siebert, F. (1997) *Z*, *E* isomerization of the α-84 phycoviolobilin chromophore of phycoerythrocyanin from *Mastigocladus laminosus* investigated by Fourier-transform infrared difference spectroscopy, *FEBS Lett. 402*, 172−176.
14. Wiegand, G., Parbel, A., Seifert, M. H., Holak, T. A., and Reuter, W. (2002) Purification, crystallization, NMR spectroscopy and biochemical analyses of α-phycoerythrocyanin peptides, *Eur. J. Biochem. 269*, 5046−5055.
15. Davis, S. J., Vener, A. V., and Vierstra, R. D. (1999) Bacteriophytochromes: Phytochrome-like photoreceptors from nonphotosynthetic eubacteria, *Science 286*, 2517−2520.
16. Karniol, B., Wagner, J. R., Walker, J. M., and Vierstra, R. D. (2005) Phylogenetic analysis of the phytochrome superfamily reveals distinct microbial subfamilies of photoreceptors, *Biochem. J. 392*, 103−116.
17. Butler, W. L., Norris, K. H., Siegelmann, K. H., and Hendricks, S. B. (1959) Detection, essay, and preliminary purification of the pigment controlling photoresponsive development in plants, *Proc. Natl. Acad. Sci. U.S.A. 45*, 1703−1708.
18. Foerstendorf, H., Benda, C., Gärtner, W., Storf, M., Scheer, H., and Siebert, F. (2001) FTIR studies of phytochrome photoreactions reveal the C═O bands of the chromophore: Consequences for its protonation states, conformation and protein interaction, *Biochemistry 40*, 14952−14959.
19. Reuter, W., and Nickel-Reuter, C. (1993) Molecular assembly of the phycobilisomes from the cyanobacterium *Mastigocladus laminosus*, *J. Photochem. Photobiol., B 18*, 51−66.

20. Berman, H. M., Westbrook, J., Feng, Z., Gilliland, G., Bhat, T. N., Weissig, H., Shindyalov, I. N., and Bourne, P. E. (2000) The Protein Data Bank, *Nucleic Acids Res. 28*, 235−242.
21. Read, R. J. (2001) Pushing the boundaries of molecular replacement with maximum likelihood, *Acta Crystallogr. D57*, 1373−1382.
22. McRee, D. E. (1999) XtalView/Xfit: A Versatile Program for Manipulating Atomic Coordinates and Electron Density, *J. Struct. Biol. 125*, 156−165.
23. Brunger, A. T., Adams, P. D., Clore, G. M., DeLano, W. L., Gros, P., Grosse-Kunstleve, R. W., Jiang, J. S., Kuszewski, J., Nilges, M., Pannu, N. S., Read, R. J., Rice, L. M., Simonson, T., and Warren, G. L. (1998) Crystallography & NMR system: A new software suite for macromolecular structure determination, *Acta Crystallogr. D54*, 905−921.
24. Bourgeois, D., Verneede, X., Adam, V., Fioravanti, E., and Ursby, T. (2002) A microspectrophotometer for UV-visible absorption and fluorescence studies of protein crystals, *J. Appl. Crystallogr. 35*, 319−326.
25. Heilbronner, E., and Bock, H. (1978) *Das HMO-Modell und seine Anwendung, Grundlagen und Handhabung*, 2nd ed., Verlag Chemie, Berlin.
26. Wagner, J. R., Brunzelle, J. S., Forest, K. T., and Vierstra, R. D. (2005) A light-sensing knot revealed by the structure of the chromophore-binding domain of phytochrome, *Nature 438*, 325−331.
27. Moffat, K. (1989) Time-resolved macromolecular crystallography, *Annu. Rev. Biophys. Chem. 18*, 309−332.
28. Schmidt, M., Rajagopal, S., Ren, Z., and Moffat, K. (2003) The application of the singular value decomposition to time-resolved X-ray data, *Biophys. J. 84*, 2112−2129.
29. Schmidt, M., Pahl, R., Ihee, H., and Srajer, V. (2005) Protein ligand interaction probed by time-resolved X-ray structure determination, in *Methods in Molecular Biology, Volume 305, Protein−Ligand Interactions: Methods and Applications* (Nienhaus, G. U., Ed.) pp 115−154, Humana Press, Totowa, NJ.
30. Scheer, H., and Kufer, W. (1977) Studies on plant bile pigments. IV. Conformational studies on C-phycocyanin from *Sprirulina platensis*, *Z. Naturforsch. 32c*, 513−519.
31. Scheer, H. (1982) Phycobiliproteins: Molecular aspects of photosynthetic antenna system, in *Light reaction path of photosynthesis* (Fong, F. K., Ed.) pp 7−45, Springer-Verlag, Berlin.
32. Makinen, M. H., and Eaton, W. A. (1974) Optically detected conformational changes in haemoglobin single crystals, *Nature 247*, 62−64.
33. Kneip, C., Parbel, A., Foerstendorf, H., Scheer, H., Siebert, F., and Hildebrandt, P. (1998) Fourier transform near-infrared resonance Raman spectroscopic study of the α-subunit of phycoerythrocyanin and phycocyanin from the cyanobacterium *Mastigocladus laminosus*, *J. Raman Spectrosc. 29*, 939−944.
34. Nield, J., Rizkallah, R. J., Barber, J., and Chayen, N. E. (2003) The 1.45 Å three dimensional structure of C-Phycocyanin from the thermophilic cyanobacterium *Synechococcus elongates*, *J. Struct. Biol. 141*, 149−155.
35. Reuter, W., Wiegand, G., Huber, R., and Than, M. E. (1999) Structural analysis at 2.2 Å of orthorhombic crystals present the asymmetry of the allophycocyanin-linker complex, AP•$L_C^{7.8}$, from phycobilisomes of *Mastigocladus laminosus*, *Proc. Natl. Acad. Sci. U.S.A. 96*, 1363−1368.
36. Andresen, M., Wahl, M. C., Stiel, A. C., Gräter, F., Schäfer, L. V., Trowitzsch, S., Weber, G., Eggeling, C., Grubmüller, H., Hell, S. W., and Jakobs, S. (2005) Structure and mechanism of the reversible photoswitch of a fluorescent protein, *Proc. Natl. Acad. Sci. U.S.A. 102*, 13070−13074.
37. Wiedenmann, J., Ivanchencko, S., Oswald, F., Schmitt, F., Röcker, C., Salih, A., Spindler, K.-D., and Nienhaus, G. U. (2004) EosFP, a fluorescent marker protein with UV-inducible green-to-red fluorescence conversion, *Proc. Natl. Acad. Sci. U.S.A. 101*, 15905−15910.
38. Friedrich, J. (1995) Hole burning spectroscopy and the physics of proteins, in *Methods of Enzymology: Biochemical Spectroscopy* (Sauer, K., Ed.) Vol. 246, pp 224−249, Academic Press, San Diego.
39. Holzwarth, A. R., Bittersmann, E., Reuter, W., and Wehrmeyer, W. (1990) Studies on chromophore coupling in isolated phycobiliproteins. III. Picosecond excited state kinetics and time-resolved fluorescence spectra of different allophycocyanins from *Mastigocladus laminosus*, *Biophys. J. 51*, 1−12.
40. Hucke, M., Schweitzer, G., Holzwarth, A. R., Sidler, W. A., and Zuber, H. (1993) Studies of chromophore coupling in isolated phycobiliproteins. IV. Femtosecond transient absorption study of ultrafast excited state dynamics in trimeric phycoerythrocyanin complexes, *Photochem. Photobiol. 57*, 76−80.
41. Lundell, D. J., and Glazer, A. N. (1981) Allophycocyanin B. A common β subunit in *Synechococcus* allophycocyanin B (λ_{max} 670 nm) and allophycocyanin (λ_{max} 650 nm), *J. Biol. Chem. 256*, 12600−12606.
42. Mroginski, M. A., Murgida, D. H., von Stetten, D., Kneip, C., Mark, F., and Hildebrandt, P. (2004) Determination of the chromophore structure in the photoinduced reaction cycle of phytochrome, *J. Am. Chem. Soc. 126*, 16734−16735.
43. Fischer, A. J., and Lagarias, J. C. (2004) Harnessing phytochromes's glowing potential, *Proc. Natl. Acad. Sci. U.S.A. 101*, 17334−17339.

BI061844J